Kevin L. Felch was born in Denver, CO in 1952. After receiving the B.A. degree in physics from Colorado College, Colorado Springs, in 1975, he attended Dartmouth College, Hanover, New Hampshire, where he received the Ph.D. degree in physics in 1980. While at Dartmouth, he carried out experiments observing the microwave Cerenkov radiation produced when a relativistic electron beam is injected into a dielectric-lined lined waveguide, and participated in various free-electron laser studies.

From 1980–1981 he spent a year doing post-doctoral research at the Laboratoire PMI of the Ecole Polytechnique, Palaiseau, France. This work involved a series of free-electron laser studies using intense relativistic electron beams, as well as investigations of the energy disposition of dense electron beams in thin foil targets. In 1981 he joined the Microwave Tube Division of Varian Associates, Inc., Palo Alto, CA, where he is a design engineer in the gyrotron program. This work is aimed at producing high power, high-frequency microwave radiation for plasma heating and communications applications.

Dr. Felch is a member of the Plasma Physics Division of the American Physical Society.

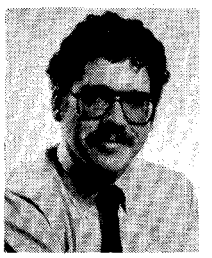

Stephen T. Spang (S'80, M'81) received the B.S.E.E. degree with distinction from Cornell University, Ithaca, N.Y., in May 1981.

While at Cornell, he was involved with the Cooperative Engineering Program. He served as a Design Engineer for bubble memories and as a Product Engineer for CMOS logic circuits at National Semiconductor. He joined the Varian Gyrotron Engineering Group in 1981 and is involved with the testing of 60-GHz oscillators and development of millimeter-wave cold test techniques for cavities, window, and waveguide components.

Mr. Spang is a member of Eta Kappa Nu.

On the Problem of Applying Mode-Matching Techniques in Analyzing Conical Waveguide Discontinuities

GRAEME L. JAMES

Abstract—**Mode-matching techniques in the past have been successfully used to analyze rectangular and circular waveguide problems involving transverse discontinuities. The extension of this method to conical waveguide discontinuities is shown to exhibit difficulties of convergence caused by the behavior of the cutoff conical modes. To illustrate the problem, the junction of a smooth-walled cylindrical waveguide with a corrugated conical horn is discussed in some detail.**

I. Introduction

THE SOLUTION to a transverse discontinuity in a rectangular or circular waveguide using mode-matching techniques has been shown to provide an accurate means of determining the properties created by the discontinuity [1]–[3]. With the properties of the single step established, it is then possible to obtain a solution for any circular or rectangular waveguide which can be considered as a number of transverse discontinuities separated by short lengths of waveguide. This is demonstrated in [4] for the junction between a cylindrical smooth-walled waveguide and a corrugated cylindrical waveguide.

A natural extension of this approach is to analyze transverse discontinuities in conical waveguides. However, in doing so, a number of difficulties arise. This will be demonstrated here by considering the example of the junction between a smooth-walled cylindrical waveguide and a corrugated conical horn. To begin, we review the technique as applied to a small-angle horn where the analysis can be carried out in terms of cylindrical waveguide modes.

II. Junction Between Cylindrical Guide and Small-Angle Corrugated Conical Horn

The radiation pattern of corrugated conical horns are characterized by low sidelobe and low cross-polarization levels. As a result, they are used extensively as feeds in high-performance low-noise reflector antenna systems. To maintain these desirable features, careful design of the throat region of the horn (i.e., the circular-to-conical waveguide junction) is crucial. If the horn semi-angle θ_0 is small

Manuscript received October 19, 1982; revised May 3, 1983.

The author is with the Division of Radiophysics, CSIRO, Sydney, Australia, RPP2660.

0018-9480/83/0900-0718$01.00 ©1983 IEEE

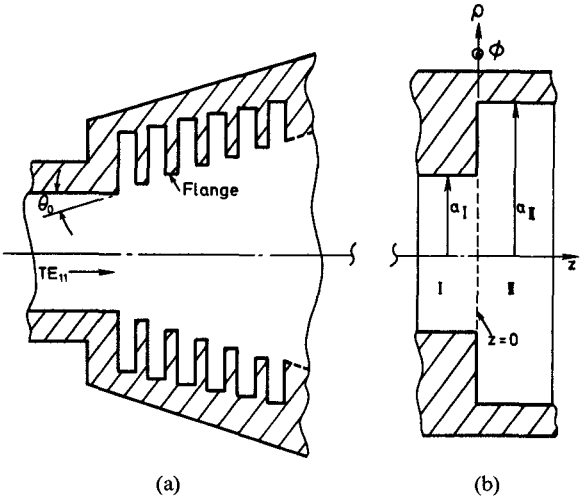

(a) (b)

Fig. 1. (a) A cross-sectional view of a cylindrical-to-corrugated conical waveguide junction for a small-angle horn. (b) The basic discontinuity problem used in analyzing the junction.

($\theta_0 \lesssim 20°$) then the slots forming the corrugated conical surface can be set normal to the axis of the horn, as shown in Fig. 1(a). The throat region of the horn can then be considered as a series of changes in circular waveguide cross section, as in Fig. 1(b), separated by short lengths of circular waveguide.

The electromagnetic field $\boldsymbol{E}, \boldsymbol{H}$ transverse to the z-direction in a circular waveguide of radius a can be represented by the modal solution (assuming here an azimuthal wavenumber of one)

$$\boldsymbol{E} = \sum_\nu (A_\nu + B_\nu)\boldsymbol{e}_\nu$$

$$\boldsymbol{H} = \sum_\nu (Y_\nu^+ A_\nu - Y_\nu^- B_\nu)\boldsymbol{h}_\nu \tag{1}$$

where $\boldsymbol{e}_\nu, \boldsymbol{h}_\nu$ are the transverse modal fields, Y_ν^+, Y_ν^- are the outward and inward wave admittances, and A_ν, B_ν are the modal coefficients. The transverse modal fields and the wave admittance are deduced from the outward and inward wave functions ψ_ν^+, ψ_ν^- given by

$$\psi_\nu^\pm = f_\nu(\rho, \phi)\exp(\mp \bar{\gamma}_\nu kz)$$

where

$$f_\nu(\rho, \phi) = J_1(X_\nu \rho/a)\begin{Bmatrix}\sin\phi \\ \cos\phi\end{Bmatrix}. \tag{2}$$

Here the value of X_ν is determined by the boundary condition at $\rho = a$ (where for TE$_{1\nu}$ modes, $J_1'(X_\nu) = 0$ and for TM$_{1\nu}$ modes, $J_1(X_\nu) = 0$). The propagation coefficient $\bar{\gamma}_\nu$ is equal to $j\Delta_\nu$ for propagating modes (when $X_\nu < ka$), and to Δ_ν for cutoff modes ($X_\nu > ka$); in each case $\Delta_\nu = |1 - (X_\nu/ka)^2|^{1/2}$. The wave admittances, normalized to the free-space admittance $\sqrt{\epsilon/\mu}$, are given by

$$Y_\nu^+ = Y_\nu^- = \Delta_\nu, \qquad x_\nu < ka$$
$$Y_\nu^+ = Y_\nu^- = -j\Delta_\nu, \qquad x_\nu > ka \tag{3a}$$

for TE$_{1\nu}$ modes and by

$$Y_\nu^+ = Y_\nu^- = 1/\Delta_\nu, \qquad x_\nu < ka$$
$$Y_\nu^+ = Y_\nu^- = j/\Delta_\nu, \qquad x_\nu > ka \tag{3b}$$

for TM$_{1\nu}$ modes.

In solving the step discontinuity problem illustrated in Fig. 1(b), we begin by representing the fields in regions I and II by the modal solution given by (1). Then by matching the fields across the common boundary at $z = 0$, we can express the solution for the unknown modal coefficients in a scatter matrix formulation as described in [4]. The scatter matrices for the changes in waveguide cross section in Fig. 1(a), together with those for the short lengths of waveguide separating them which go to make up the slots and flanges of the corrugated surface (the scatter matrix for a length of waveguide is trivially obtained), are progressively cascaded through the horn to determine its electromagnetic behavior. This technique discussed in [4] is applied in [5] to small-angle corrugated horns of the type shown in Fig. 1(a). The method has also been extended to analyze the effect of ring-loaded slots [5], [6], but for our purposes here we need only consider conventional slots, as in Fig. 1(a).

III. Junction Between Cylindrical Guide and Large-Angle Corrugated Conical Horn

When the horn semi-angle is much greater than 20°, then it is more usual and desirable to set the slots normal to the conical surface, as shown in Fig. 2(a). To analyze this problem by the above method we approximate the slots (and flanges) by changes in conical waveguide cross section separated by short lengths of conical waveguide. This is illustrated in Fig. 2(b) for a single slot. Thus the basic discontinuity to be solved is shown in Fig. 2(c): it is necessary to determine the scatter matrix through the junction at radius r_0, between two smooth-walled conical waveguides having differing angles. As before, we express the field in regions I and II of Fig. 2(c) by the modal solution given by (1). For a conical waveguide the wave functions $\psi_\nu^\pm$ are given by

$$\psi_\nu^\pm = g_\nu(\theta, \phi)\hat{H}_\nu^{(2)(1)}(kr) \tag{4}$$

where

$$g_\nu(\theta, \phi) = P_\nu^1(\cos\theta)\begin{Bmatrix}\sin\phi \\ \cos\phi\end{Bmatrix}.$$

For values of horn semi-angle $\theta_0 \lesssim 60°$ we can use the approximation to the Legendre function given by $P_\nu^1(\cos\theta) \approx -\sigma J_1(X_\nu\theta/\theta_0)$ where $\sigma = X_\nu/\theta_0 = \nu + 1/2$ and X_ν is as defined above for cylindrical waveguides. With this approximation $g_\nu(\theta, \phi)$ is similar in form to $f_\nu(\rho, \phi)$ for cylindrical waveguides. As a result, the integrals involving cross-products of the transverse fields that occur in the solution for the waveguide discontinuity can (for the conical waveguide case) be obtained (with the exception of a constant) directly from the solutions given in [4] with a_I, a_{II} replaced by θ_0, θ_1.

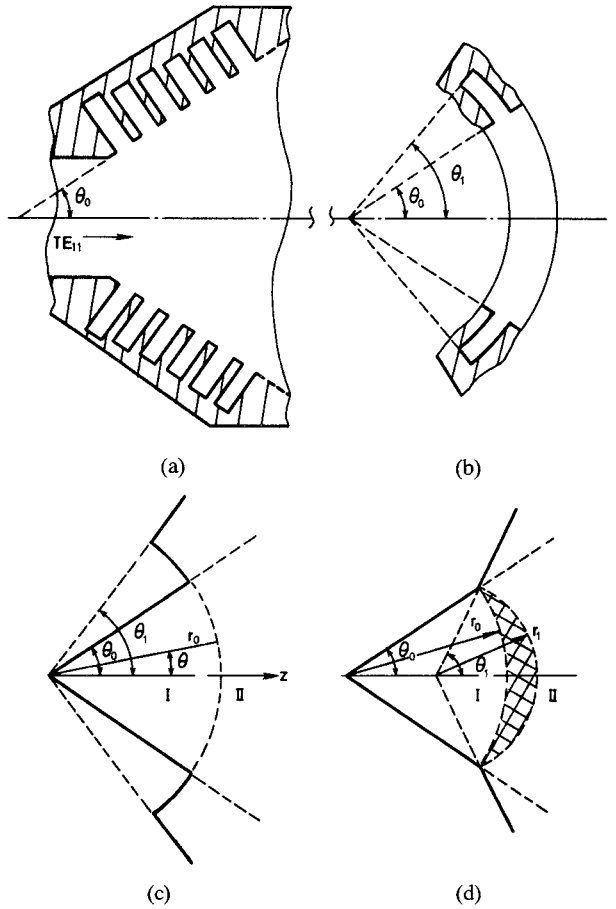

Fig. 2. Cross-sectional view of (a) cylindrical-to-corrugated conical waveguide junction for a large-angle horn; with (b) the approximation used for the slots; and (c), (d) the basic discontinuity problems used in analyzing the junction.

The main, and crucial, difference between the two cases is in the propagation behavior in the direction normal to the transverse fields. If we can assume that kr is large, the uniform asymptotic expansion of the spherical Hankel function can be used in the conical waveguide mode function. Thus we have

$$\hat{H}_\nu^{(1)(2)}(kr) = \hat{J}_\nu(kr) \pm j\hat{N}_\nu(kr) \sim \left[\frac{\pi^2\tau}{(\sigma/kr)^2-1}\right]^{1/4} [Ai(\tau) \mp jBi(\tau)] \quad (5)$$

where

$$\sigma = \nu + 1/2, \tau = -\sigma^{2/3}\xi$$

and

$$2/3\xi^{3/2} = \begin{cases} \left(\left[(kr/\sigma)^2-1\right]^{1/2} - \cos^{-1}(\sigma/kr)\right), \\ \qquad kr/\sigma > 1 \\ \exp(j3\pi/2)\left(j\cos^{-1}(\sigma/kr)\right. \\ \quad \left. -\left[1-(kr/\sigma)^2\right]^{1/2}\right), \qquad kr/\sigma < 1. \end{cases}$$

The normalized wave admittances for $TE_{1\nu}$ modes in the conical waveguide are

$$Y_\nu^+ = j\hat{H}_\nu^{(2)\prime}(kr)/\hat{H}_\nu^{(2)}(kr) \quad Y_\nu^- = -j\hat{H}_\nu^{(1)\prime}(kr)/\hat{H}_\nu^{(1)}(kr) \quad (6)$$

and for $TM_{1\nu}$ modes the wave admittances are given by the inverse of these expressions. Making use of (5) we can write the $TE_{1\nu}$ mode admittances as

$$Y_\nu^\pm = \Delta_\nu \left\{ \frac{1}{|\tau|^{1/2}} \frac{Bi'(\tau) \mp jAi'(\tau)}{Ai(\tau) \pm jBi(\tau)} \right\} \quad (7)$$

where we interpret the value of ka in Δ_ν as equal to $kr\theta_0$. For modes that are strongly propagating the term inside the curly bracket, (7) reduces to unity and consequently the wave impedances are similar to the cylindrical waveguide result given by (3). For modes that are strongly cutoff, $\tau > 1$ and (7) becomes

$$Y_\nu^\pm = \Delta_\nu e^{-4/3\tau^{3/2}} \mp j\Delta_\nu, \qquad TE_{1\nu} \text{ modes}$$

$$Y_\nu^\pm = \frac{1}{\Delta_\nu} e^{-4/3\tau^{3/2}} \pm j/\Delta_\nu, \qquad TM_{1\nu} \text{ modes.} \quad (8)$$

As is well known, the mode in cylindrical waveguides is abruptly cut off when $X_\nu = ka$, with the wave admittance changing from being purely conductive to being purely susceptive, whereas in conical waveguides there is no well-defined cutoff but rather a cutoff radius at $kr = \sigma$, where the wave admittance changes from being predominantly conductive to being predominantly susceptive. Another important difference between cylindrical and conical waveguides is that for the latter case any outward cutoff mode which is generated decays exponentially away from the discontinuity (as in a cylindrical waveguide) while any inward cutoff mode generated *increases* exponentially towards the apex of the cone.

Before we see how these features of conical waveguide mode propagation affect our results, there is the additional problem of the junction between two conical waveguides having the same diameter but with different angles, as shown in Fig. 2(d). The scatter matrix solution to this problem is necessary for the input junction from the circular waveguide (where $\theta_0 = 0$) and also allows for any flaring (i.e., increasing θ_0) along the horn. If $\theta_1 > \theta_0$, as in Fig. 2(d) then, as pointed out in [7], a direct mode-matching procedure is, strictly, not applicable, since neither modal expansion for the two conical waveguides is valid in the hatched segment shown in the figure. (Note that if $\theta_1 < \theta_0$, this problem does not arise, since the two waveguides share a common area where both modal expansions are valid.) For a rigorous formulation, it is necessary to provide the segment with its own field representation [7], and this can lead to some formidable mathematical problems [8]. However, if θ_1 is not very much greater than θ_0, we can arrive at an approximate solution by continuing the modal expansion of the field in region I beyond its strict range of validity to the spherical cap at $r = r_1$ where we match the transverse fields with those for region II.

We now consider the procedure for mode matching up to the first slot for the waveguide junction problem given in Fig. 2(a). As an example we have chosen $\theta_0 \approx 30°$ with input circular waveguide radius $a_0/\lambda \approx 0.35$. For this case the cutoff circles, where $X_\nu = kr\theta_0$ are shown in Fig. 3 for the first three modes. As described above, the field can be progressively matched at the boundaries U, V, and W shown in the figure. Consider now the behavior of the first three modes when excited at the V-boundary. Any TE_{11} outward and inward modes excited at V will be strongly propagating and behave in a similar way to this mode in a cylindrical waveguide. This will be true even for the inward wave which arrives at the boundary at U, since the TE_{11} mode is not near cutoff when it reaches this junction.

Any TE_{12} outward mode excited at V will initially decay exponentially away from the boundary with a mainly susceptive wave admittance as given in (8). As the TE_{12} cutoff circle is approached the propagation behavior will become more complex, with the wave admittance given by (7). However, any TE_{12} inward wave generated at V will remain cut off and (considered alone) will increase exponentially towards the boundary at U. For the total TE_{12} mode field in the section of waveguide U–V to remain bounded, it is necessary for the waveguide junction at U to present essentially a short circuit to this mode. The analysis of this junction yields $A_u = -B_u$ for all strongly cutoff modes, thereby fulfilling the requirement that these modes be bounded. This also applies to the TM_{11} inward mode. Although at V the TM_{11} mode can propagate, it is strongly cut off by the time it reaches the boundary at U. For these two modes the analysis yields, as before, $A_u = -B_u$ and a standing wave exists to the left of the V boundary. The admittance of the TE_{12} wave Y_ν at V is, therefore, deduced to be

$$Y_\nu = j\frac{\hat{N}_\nu'(kr_v)\hat{J}_\nu(kr_u) - \hat{N}_\nu(kr_u)\hat{J}_\nu'(kr_v)}{\hat{N}_\nu(kr_v)\hat{J}_\nu(kr_u) - \hat{N}_\nu(kr_u)\hat{J}_\nu(kr_v)} \tag{9}$$

and the admittance for the TM_{11} mode is given by the inverse of this expression. If the two boundaries are well separated, then $\hat{J}_\nu(kr_u) \ll \hat{J}_\nu'(kr_v)$ and the admittance given by (9) reduces to

$$Y_\nu = j\hat{J}_\nu'(kr_v)/\hat{J}_\nu(kr_v). \tag{10}$$

In the expression for the admittance given by (9), there are terms which are exponentially large (viz. $\hat{N}_\nu(kr_u)$) and terms which are exponentially small (viz. $\hat{J}_\nu(kr_u)$). Herein lies the difficulty in successfully analyzing problems such as those illustrated in Fig. 3 by mode-matching methods.

Similar difficulties were encountered by Sporleder and Unger [9] in a traveling-wave coupled-wave equation analysis of tapered-horn junctions. In their solution, they substituted for cutoff inward waves the wave admittance given by (6) with that given by (10). This approach would appear to be questionable on at least two counts. First, the impedance given by (10) is not for a traveling-wave representation but is the result of the combination of the inward and outward waves. Second, there is no indication in [9] of how

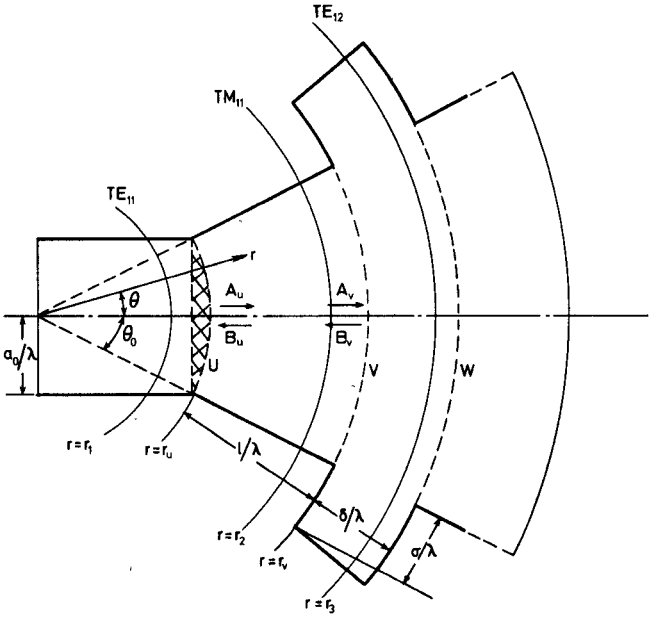

Fig. 3. Cross-sectional view of the cylindrical-to-conical waveguide junction having a single slot in the horn.

to effect a smooth change from (10) to (6) when in the vicinity of the cutoff radius. This would occur, for example, if the input-wave radius a_0 increased so that the TM_{11} cutoff radius r_2 was at or close to the radius r_u of the U boundary.

To illustrate some of the problems encountered in conical waveguide matching we will consider the results for two examples.

A. Cylindrical Guide to Conical Guide with a Single Step

Referring to Fig. 3, let us assume $l/\lambda = 0$, $\delta/\lambda = \infty$, $a_0/\lambda = 0.84$, and $\sigma/\lambda = 0.5$. With these dimensions, the circular waveguide can propagate both the TE_{11} and TM_{11} mode. Assume the TE_{11} mode only is initially excited in the cylindrical waveguide. We wish to determine the TE_{11} mode return loss from the junction as a function of the number M of input waveguide modes used in the analysis. Consider now the case where θ_0 is limited to 6°. For such a small angle the return loss result should be similar to the cylindrical waveguide case ($\theta_0 = 0°$), which can be solved accurately [1]–[4], and hence can be used to check the accuracy of the small-angle conical-horn result. The case then where $\theta_0 = 0°$ is shown in Fig. 4, and is seen to have converged for $M \geqslant 8$. The corresponding result for $\theta_0 = 6°$ is shown by curve (i) in the figure. For $M \geqslant 3$, the conical waveguide modes are strongly cut off, and it is seen that by the time the sixth mode has been included the solution has become unstable owing to the numerical difficulties of dealing with large and small quantities in the one expression, as discussed above in relation to (9). For strongly cutoff mode $\hat{J}_\nu(kr_u) \propto e^{-2/3\tau^{3/2}}$ and $\hat{N}_\nu(kr_u) \propto e^{2/3\tau^{3/2}}$. In the present example we have for the first cutoff mode ($M = 3$) $\tau \approx 3$ and for the second cutoff mode $\tau \approx 6.5$, which gives a difference of nearly 10 orders of magnitude

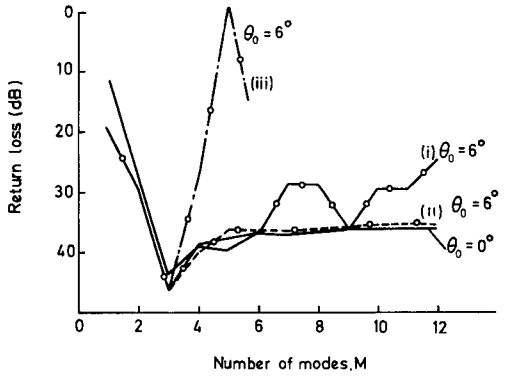

Fig. 4. TE_{11} mode return loss as a function of the number of modes M considered in the input cylindrical waveguide of Fig. 3 with $l/\lambda = 0$, $\delta/\lambda = \infty$, $\sigma/\lambda = 0.5$, $a_0/\lambda = 0.84$ and values of θ_0, 0°, and 6°.

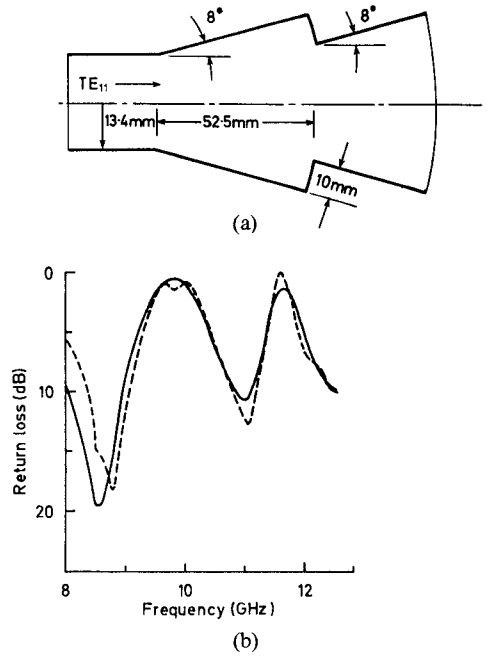

Fig. 5. (a) Cross-sectional view of a cylindrical-to-conical waveguide junction. (b) Comparison of the measured (----) and theoretical (——) values for the TE_{11} mode return loss of the junction in (a).

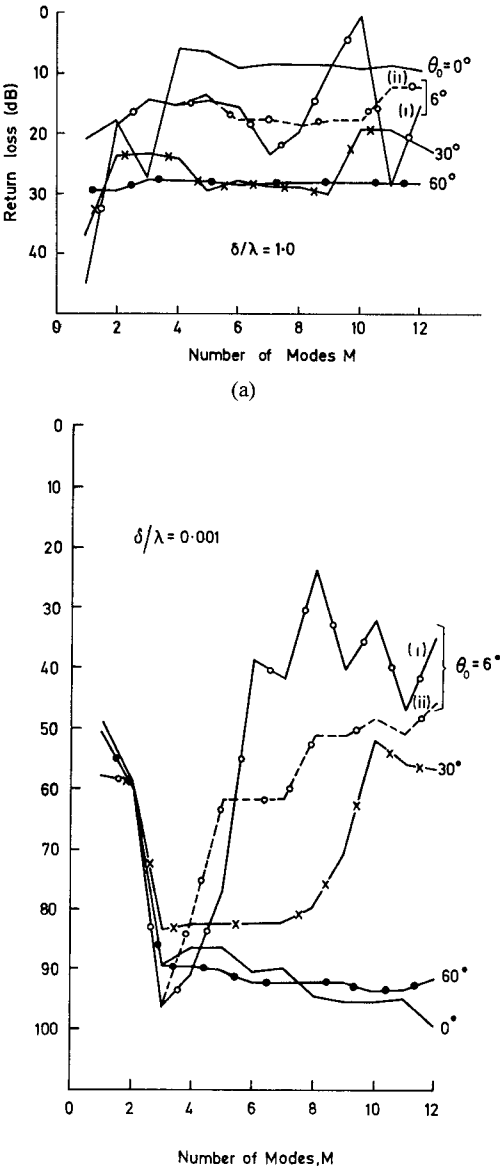

Fig. 6. TE_{11} mode return loss for various values of θ_0 for the waveguide shown in Fig. 3 where $l/\lambda = 0$, $\sigma/\lambda = 0.5$, $a_0/\lambda = 0.84$. (a) $\delta/\lambda = 1$. (b) $\delta/\lambda = 0.001$.

between the spherical Bessel and spherical Neumann functions. To highlight the importance of retaining the numerically small spherical Bessel function term in the solution, refer to (8) for the wave admittance of strongly cutoff modes. If we are tempted to ignore the real component as being insignificant, then the result for the return loss is given by curve (iii) in Fig. 4, which of course yields a totally erroneous result. If we artificially limit the magnitude of τ to the value of the first strongly cutoff mode, then we get the result given by curve (ii), which converges to around the expected value of the return loss.

As a further check on the solution, we measured the TE_{11} mode return loss for the conical-horn step problem as shown in Fig. 5. By limiting the magnitude of τ for strongly cutoff modes (as in curve (ii) of Fig. 4), it is seen that generally very good agreement exists between theory and experiment. The theoretical results shown are for $M = 4$ but little variation from this result occurred by taking up to 12 modes in the analysis.

B. Cylindrical Guide to Conical Guide with a Single Slot

We will now consider the analysis for a single slot and also consider larger values of horn angles. Referring to Fig. 3, let us assume (as in the first example) $l/\lambda = 0$, $a_0/\lambda = 0.84$, and $\sigma/\lambda = 0.5$, but let δ/λ be fixed at 1 and 0.001, and $0° \leqslant \theta_0 \leqslant 60°$. The return loss convergence is plotted in Fig. 6 as a function of M. As before, we have also given the cylindrical waveguide analysis result ($\theta_0 = 0$), and when $\delta/\lambda = 1$ (Fig. 6(a)), this result is seen to converge for $M \geqslant 8$. When $\theta_0 = 6°$, the result becomes unstable after six modes (curve (i)). (This is similar to the example shown in Fig. 4.) By artificially limiting the value of τ, the result (curve (ii)) appears satisfactory up to 10 modes but then it

also becomes unstable. As the angle θ_0 is increased the conical modes are less strongly cut off. This is demonstrated in Fig. 6(a), where for $\theta_0 = 30°$ the solution only becomes unstable for $M > 9$ and for $\theta_0 = 60°$ the solution has remained stable for up to the 12 modes considered. When the slot width is made very narrow, as in Fig. 6(b), the instability of the conical mode-matching solution is clearly evident. When $\theta_0 = 6°$, limiting the value of τ (curve (ii)) does not prevent the solution from going wildly unstable as the strongly cutoff modes are included in the solution. As before, the instability is delayed for larger angle horns, occurring when $M > 8$ for $\theta_0 = 30°$ and when $M > 12$ (not shown) for $\theta_0 = 60°$.

IV. Conclusion

It has been demonstrated that mode matching at discontinuities in conical waveguides is severely restricted by the behavior of the strongly cutoff conical modes directed towards the apex of the horn. For large values of horn semi-angle θ_0, the problem becomes less severe, to the extent that mode-matching techniques as given here could be used successfully. However, more attention is needed to solve the problem posed by the cylindrical waveguide to conical-guide junction when θ_0 is large, since the commonly used mode-matching method cannot be considered reliable.

References

[1] A. Wexler, "Solution of waveguide discontinuities by modal analysis," *IEEE Trans. Microwave Theory Tech.*, vol. MTT-15, pp. 508–517, 1967.

[2] W. J. English, "The circular waveguide step-discontinuity mode transducer," *IEEE Trans. Microwave Theory Tech.*, vol. MTT-21, pp. 633–636, 1973.

[3] P. H. Masterman and P. J. B. Clarricoats, "Computer field-matching solution of waveguide transverse discontinuities," in *Proc. Inst. Elec. Eng.*, vol. 118, 1971, pp. 51–63.

[4] G. L. James, "Analysis of design of TE_{11}-to-HE_{11} corrugated cylindrical waveguide mode converters," *IEEE Trans. Microwave Theory Tech.*, vol. MTT-29, pp. 1059–1066, 1981.

[5] ——, "TE_{11}-to-HE_{11} mode converters for small-angle corrugated horns," *IEEE Trans. Antennas Propagat.*, vol. AP-30, no. 6, pp. 1057–1062, Nov. 1982.

[6] G. L. James and B. M. Thomas, "TE_{11} to He_{11} cylindrical waveguide mode converters using ring-loaded slots," *IEEE Trans. Microwave Theory Tech.*, vol. MTT-30, pp. 278–285, 1982.

[7] L. Lewin, "On the inadequacy of discrete mode-matching techniques in some waveguide discontinuity problems," *IEEE Trans. Microwave Theory Tech.*, vol. MTT-18, pp. 364–372, 1970.

[8] V. Daniele, M. Orefice and R. Zich, "Mode coupling coefficients in conical horn junction," in *IEEE AP-S Int. Symp. Dig.*, pp. 233–236, 1981.

[9] F. Sporleder and H.-G. Unger, *Waveguide Tapers, Transitions and Couplers*, London, England: Peregrinus, 1979, pp. 117–119.

Graeme L. James was born in Dunedin, New Zealand, in 1945. He received the B.E. and Ph.D. degrees in electrical engineering from the University of Canterbury, Christchurch, New Zealand, in 1970 and 1973, respectively.

Between 1973 and 1976 he was a post-doctoral fellow with the Department of Electrical and Electronic Engineering, Queen Mary College, London, England, where he was involved in a number of projects concerned with electromagnetic scattering and diffraction. Since June 1976 he has been with the Division of Radiophysics, CSIRO, Sydney, Australia, where he has been mainly concerned with research into high-performance microwave antennas.